Research Square

Preprints are preliminary reports that have not undergone peer review.
They should not be considered conclusive, used to inform clinical practice,
or referenced by the media as validated information.

Comparative LC-MS/MS profiling of molecular features in Antarctic bacteria

José Aparecido Ferreira de Lima
Instituto Butantan
Paulo Henrique Lima
paulo.henrique@fundacaobutantan.org.br
Instituto Butantan
Daniel Carvalho Pimenta
Instituto Butantan
Alexandre Soares Rosado
King Abdullah University of Science and Technology
Adalberto Pessoa
Universidade de São Paulo

Research Article

Keywords: Antarctic bacteria, molecular profiling, LC-MS/MS, carotenoid-associated features, lipid-associated features

Posted Date: November 17th, 2026

DOI: https://doi.org/10.21203/rs.3.rs-11434543/v1

License: This work is licensed under a Creative Commons Attribution 4.0 International License.
Read Full License

Additional Declarations: No competing interests reported.

Comparative LC-MS/MS profiling of molecular features in Antarctic bacteria

Affiliations:

[1]Laboratory of Ecology and Evolution, Butantan Institute, São Paulo, SP, Brazil

[2]Laboratory of Pharmacology, Butantan Institute, São Paulo, SP, Brazil

[3]Biochemical-Pharmaceutical Technology, School of Pharmaceutical Sciences, University of São Paulo, São Paulo, SP, Brazil

[4]Biological and Environmental Sciences and Engineering (BESE), King Abdullah University of Science and Technology (KAUST), Thuwal, Kingdom of Saudi Arabia

Authors:

José Aparecido Ferreira de Lima[1], Paulo Henrique Lima[2,3], Daniel Carvalho Pimenta[2], Alexandre Soares Rosado[4], Adalberto Pessoa[3]

Author Contributions

AP: Conceptualization, supervision, data interpretation, writing—review and editing, and final approval of the manuscript. DCP: Data interpretation, literature review, writing—review and editing, and final approval of the manuscript. JAFL: Data analysis, data interpretation, literature review, and writing—review and editing. PHL: Conceptualization, data analysis, data interpretation, literature review, writing—original draft, and writing—review and editing. ASR: Data analysis, data interpretation, literature review, and writing—review and editing. All authors read and approved the final version of the manuscript and agreed to be accountable for all aspects of the work.

Acknowledgments

The authors gratefully acknowledge the Butantan Institute (São Paulo, Brazil) and the Butantan Foundation for institutional support and valuable contributions to this work.

Corresponding author:

Paulo Henrique Lima
Laboratory of Pharmacology, Butantan Institute
Av. Vital Brasil, 1500, Butantã, São Paulo, SP 05503-900, Brazil
Telephone: +55 (11) 2627-9742
E-mail: paulo.henrique@fundacaobutantan.org.br

Abstract

This study compared selected molecular features in methanolic extracts from five Antarctic bacterial isolates: *Arthrobacter cryoconiti* LAP 167 (A1), *Pseudomonas* sp. AT LP67 (B1), *Microbacterium* sp. LEMMJ01 (C7), and two *Arthrobacter agilis* isolates (F1 and G1). Liquid chromatography–mass spectrometry (LC-MS) and liquid chromatography–high-resolution quadrupole time-of-flight tandem mass spectrometry (LC-HR-Q-TOF-MS/MS) were used to compare precursor-ion mass-to-charge ratios (*m/z*), chromatographic retention times, and available product-ion profiles. An analytical β-carotene standard was examined under the same conditions. A molecular feature near *m/z* 741.578 was detected in both *A. agilis* isolates, with closely matching precursor-ion masses, retention times, and a reported product ion. Features near *m/z* 535.470 were observed in C7, G1, and F1, but differences in retention times and reported product-ion profiles prevented their assignment to a common molecular structure. An additional feature near *m/z* 537.486 was detected in four of the five isolates, whereas features near *m/z* 523.470, 521.455, and 509.455 occurred in subsets of the isolate collection. Comparison with the β-carotene reference distinguished the bacterial signal near *m/z* 537.486 from the standard under the analytical conditions employed. The available evidence did not establish specific carotenoid structures, C40 or C50 classifications, or individual diacylglycerol species. Overall, the comparative analysis revealed overlapping but differentiated distributions of selected molecular features and demonstrated the importance of integrating chromatographic retention and tandem mass spectrometry when evaluating analytical correspondence across bacterial isolates. These findings provide a comparative basis for prioritizing molecular features for further structural characterization.

Key Points

Antarctic isolates showed distinct distributions of selected molecular features.

Similar precursor masses did not consistently match retention and MS/MS profiles.

Comparative LC-MS/MS prioritized unresolved features for structural characterization.

Keywords: Antarctic bacteria; molecular profiling; LC-MS/MS; carotenoid-associated features; lipid-associated features.

Introduction

Bacterial carotenoids comprise a structurally diverse group of pigments with important biological functions and biotechnological applications. Variation in isoprenoid chain length, degree of unsaturation, configuration, and structural modification gives rise to C30, C40, and C50 carotenoids and related derivatives (Maoka 2023; Polyakov et al. 2023; López et al. 2023). Microorganisms from extreme environments harbor diverse carotenoid profiles, and Antarctic bacteria have been reported to produce C40 and C50 carotenoids, including β-carotene, zeaxanthin, β-cryptoxanthin, lycopene, and bacterioruberin-associated compounds (Ashokkumar et al. 2023; Vila et al. 2019; Pradel et al. 2021; Styczynski et al. 2020; Korkerd et al. 2024). Carotenoid production has also been described in Antarctic *Arthrobacter* and *Microbacterium* isolates, including *Microbacterium* sp. LEMMJ01 (Reis-Mansur et al. 2019; Flegler and Lipski 2022; Noby et al. 2023; Paredes Contreras et al. 2025).

The Antarctic environment provides an important setting for investigating microbial molecular diversity under extreme environmental conditions. In addition to carotenoids, bacterial extracts contain lipid-associated molecular features that contribute to their chemical complexity and provide complementary information on microbial molecular composition (Akulava et al. 2024; Scales et al. 2024). Although carotenoid profiles have been reported for individual Antarctic bacterial isolates, the comparative distribution of carotenoid- and lipid-associated molecular features across isolates remains less explored. Comparative molecular profiling can help distinguish recurring signals from isolate-associated features, reveal analytical similarities and differences, and prioritize candidate molecules for subsequent characterization.

The characterization of structurally related compounds requires complementary analytical evidence because distinct molecular species may exhibit similar precursor-ion masses. Accordingly, precursor-ion *m/z*, chromatographic behavior, and tandem mass spectrometry (MS/MS) fragmentation patterns should be considered together when evaluating molecular features and supporting tentative annotations (Azevedo-Meleiro and Rodriguez-Amaya 2004; Rivera et al. 2014; Maoka 2023; López et al. 2023; Sandmann 2022). Similar precursor-ion masses alone do not establish molecular identity, and differences in chromatographic behavior or product-ion patterns may indicate that apparently related signals represent distinct chemical entities. Comparison with authentic

reference standards can provide additional analytical context, although structural assignments must remain consistent with the evidence available.

In this study, five Antarctic bacterial isolates—*Arthrobacter cryoconiti* LAP 167 (A1), *Pseudomonas* sp. AT LP67 (B1), *Microbacterium* sp. LEMMJ01 (C7), and two *Arthrobacter agilis* isolates (F1 and G1)—were comparatively investigated using liquid chromatography–mass spectrometry (LC-MS) and liquid chromatography–high-resolution quadrupole time-of-flight tandem mass spectrometry (LC-HR-Q-TOF-MS/MS). The aim of this study was to characterize and compare the distribution of detected molecular features across the five isolates and to assess the extent to which precursor-ion *m/z*, chromatographic behavior, and available MS/MS fragmentation patterns supported analytical similarities, differences, and tentative chemical interpretations. A β-carotene reference standard was analyzed for comparison. By distinguishing recurring signals from isolate-associated features and avoiding definitive structural assignments where the evidence was insufficient, this study provides a comparative overview of molecular diversity among Antarctic bacterial isolates and prioritizes selected features for further structural characterization.

Materials and Methods

Bacterial strains and origin

Five Antarctic bacterial isolates were investigated: *Arthrobacter cryoconiti* LAP 167 (A1), *Pseudomonas* sp. AT LP67 (B1), *Microbacterium* sp. LEMMJ01 (C7), and two *Arthrobacter agilis* isolates designated F1 and G1. Isolates A1, B1, and C7 belong to the Antarctic bacterial collection maintained at the Laboratory of Molecular Microbial Ecology (LEMM), Institute of Microbiology Paulo de Góes, Federal University of Rio de Janeiro (UFRJ), Brazil. This collection was described by da Silva et al. (2017), who reported bacteria isolated from Antarctic soils and plant-associated environments. Isolates A1 (*A. cryoconiti* LAP 167) and B1 (*Pseudomonas* sp. AT LP67) originated from environmental samples collected in the Admiralty Bay region of King George Island, South Shetland Islands, Antarctica, during the austral summer of 2006/2007. The specific sampling sites for these two isolates could not be established from the available collection records. The 16S rRNA gene sequences reported by da Silva et al. (2017) are deposited in GenBank under accession numbers KX354837–KX354932. *Microbacterium* sp.

LEMMJ01 (C7) was isolated from ornithogenic soil collected near an Adélie penguin (*Pygoscelis adeliae*) nest in the vicinity of Arctowski Station, Admiralty Bay, King George Island. Its draft genome sequence is deposited in GenBank under accession number NCTV00000000 (version NCTV01000000; Schultz et al., 2017). Isolates F1 and G1 are registered in the Brazilian Collection of Microorganisms from Environment and Industry (CBMAI), maintained at the Center for Chemical, Biological and Agricultural Research (CPQBA), University of Campinas (UNICAMP), Brazil. F1 corresponds to CBMAI 1053 and was originally designated API 21 (B10), whereas G1 corresponds to CBMAI 1055 and was originally designated API 23 (B16). Both isolates were recovered from biofilms in a meltwater stream at Ginger Lake, Admiralty Bay, King George Island, Antarctica, in February 2007. The expedition identifier was not available in the collection records. Working cultures of all five isolates were maintained at the Butantan Institute, São Paulo, Brazil, and used in the experiments described in this study. The isolates are available to qualified researchers upon reasonable request.

Bacterial reactivation and cultivation

The bacterial isolates were reactivated on solid Luria–Bertani (LB) medium prepared according to Bertani (1951) and incubated at 20 °C for 120 h. Three independent biological replicates were prepared for each bacterial isolate. A single isolated colony from each strain was transferred to 50 mL of liquid LB medium in 500-mL Erlenmeyer flasks. The cultures were incubated at 20 °C and 150 rpm for 120 h. At the end of the cultivation period, the bacterial biomass was recovered and subjected to methanolic extraction.

Preparation of methanolic extracts

For each strain, a 50-mL culture aliquot was centrifuged at 2,516 ×g and 4 °C for 10 min to recover the cellular biomass. The supernatant was discarded, and the cell pellet was washed three consecutive times with ultra-pure water. After each washing step, the cells were recovered by centrifugation at 2,516×g and 4 °C for 10 min. Following the final washing step, 4 mL of chilled methanol was added to the cell pellet. The biomass was thoroughly resuspended in methanol and maintained at 20 °C for 24 h to promote extraction of methanol-soluble pigments and other intracellular metabolites. The extracts were subsequently centrifuged at 10,062 ×g and 4 °C for 10 min, and the resulting supernatants were collected. The methanolic extracts were concentrated to dryness by

96 solvent evaporation. The dried extracts were weighed and redissolved in HPLC-grade
97 methanol to a final concentration of 1 $mg.mL^{-1}$. Before chromatographic analysis, the
98 resulting solutions were passed through 0.22 µm membrane filters.

99 **LC-MS screening**

100 An initial qualitative molecular screening of the methanolic extracts was
101 performed using an LC-MS-2050 system (Shimadzu Corporation, Japan) equipped with
102 a Kinetex C18 column (50 × 2.1 mm, 5 µm) (Phenomenex, Torrance, CA, USA)
103 maintained at 40 °C. Mobile phase A consisted of water containing 0.1% acetic acid,
104 whereas mobile phase B consisted of acetonitrile containing 0.1% acetic acid. The
105 chromatographic program was 60% B from 0 to 10 min, followed by a linear increase
106 from 60 to 100% B from 10 to 25 min and an isocratic period at 100% B from 25 to 35
107 min. The flow rate was 0.2 $mL.min^{-1}$. Ionization was performed in positive mode using a
108 dual ionization source combining electrospray ionization and atmospheric-pressure
109 chemical ionization. The capillary voltage was set to 1.3 kV, the source temperature to
110 200 °C, and the nebulizing gas flow rate to 2 $L.min^{-1}$. Data were acquired in SCAN mode
111 over the *m/z* range of 150–1000. The LC-MS analysis was used as an initial qualitative
112 screening step to characterize the chromatographic and mass-spectrometric profiles of the
113 bacterial extracts and to identify molecular features for subsequent high-resolution
114 analysis.

115 **LC-HR-Q-TOF-MS/MS analysis**

116 The methanolic extracts were subsequently analyzed by liquid chromatography
117 coupled with high-resolution quadrupole time-of-flight tandem mass spectrometry (LC-
118 HR-Q-TOF-MS/MS). Chromatographic separation was performed using an Elute+ UPLC
119 system coupled to an Impact II Q-TOF mass spectrometer (Bruker Daltonics GmbH &
120 Co. KG, Bremen, Germany). A Kinetex C18 column (50 × 2.1 mm, 5 µm) maintained at
121 40 °C was used under the same mobile-phase composition, chromatographic gradient,
122 and flow rate described for the LC-MS screening analysis. Ionization was performed in
123 positive mode using a VIP-HESI-APCI source. The nebulizer pressure was set to 3.0 bar,
124 the capillary voltage to 1,000 V, the drying-gas temperature to 200 °C, the drying-gas
125 flow rate to 6.0 L min^{-1}, and the end-plate offset to −500 V. The Focus parameter was
126 active throughout the analyses. Mass spectra were acquired in data-dependent acquisition
127 (DDA) mode over an *m/z* range of 200–1300. During data acquisition, the divert valve

was directed to waste. The ion energy in MS mode was set to 5.0 eV, the collision energy to 5.0 eV, the collision-cell radio-frequency amplitude to 1200 Vpp, the transfer time to 80.0 µs, and the PrePulseStorage time to 12.0 µs. External mass calibration was performed using sodium formate. Molecular features were evaluated based on precursor-ion *m/z*, chromatographic retention behavior, and available MS/MS fragmentation patterns.

β-Carotene standard analysis

A β-carotene analytical standard (95% purity; Sigma-Aldrich, Darmstadt, Germany) was prepared at 1 mg mL^{-1} in methanol and analyzed using the LC-HR-Q-TOF-MS/MS method described in the "LC-HR-Q-TOF-MS/MS analysis" section. The standard exhibited a reported precursor ion at *m/z* 537.4441 and a retention time of 25.82 min. These measurements were used as analytical reference parameters for comparison with molecular features detected in the bacterial extracts.

HRMS data processing

MZmine version 4.10.6 (Schmid et al., 2023) was used to generate and examine the mass spectra evaluated in this study. The software was not used for automated feature detection, chromatographic peak alignment, deconvolution, or molecular annotation. Selected molecular features were evaluated using the precursor-ion *m/z*, chromatographic retention time, and available MS/MS product-ion profiles. Their occurrence across the five isolates was compared descriptively, with particular attention to recurrent signals and signals exhibiting similar precursor-ion masses but different chromatographic or fragmentation characteristics. The analysis was exploratory and focused on selected molecular features rather than comprehensive untargeted metabolomic profiling. Similarity in precursor-ion mass alone was not considered sufficient to establish molecular identity.

Molecular annotation

Molecular features detected near *m/z* 535.470 were retained as unresolved features because the available mass spectrometric evidence was insufficient to establish their molecular formulas. The previously considered formula $C_{40}H_{54}$ was rejected because its theoretical protonated-ion value, calculated as $[M+H]^+$, is approximately *m/z* 535.4298,

158 which differs from the reported precursor-ion measurements near *m/z* 535.470 by
159 approximately 0.0402 Da (approximately 75 ppm). The reported measurements therefore
160 do not support assigning these features to $C_{40}H_{54}$ or classifying them as C_{40} carotenoids.
161 The source of the mass discrepancy could not be established from the available records;
162 accordingly, no specific cause, such as transcription error, calibration error, or incorrect
163 ion assignment, is inferred. The features were retained as unresolved, without a definitive
164 molecular-formula or compound-class assignment.

165 **Data analysis and comparison**

166 The five bacterial isolates were compared descriptively using selected molecular
167 features reported in the LC-MS and LC-HR-Q-TOF-MS/MS datasets. The comparison
168 considered precursor-ion mass-to-charge ratio (*m/z*), available chromatographic retention
169 information, MS/MS product-ion profiles, and the attribution of each recorded signal to
170 the corresponding isolate. Three independent biological replicates were prepared for each
171 isolate, as described in the "Bacterial reactivation and cultivation" section. MZmine
172 version 4.10.6 was used to generate and examine the mass spectra considered in the
173 analysis; automated feature detection, chromatographic peak alignment, deconvolution,
174 and molecular annotation were not performed using this software. The analysis was
175 restricted to selected molecular features for which analytical records were available.
176 Signals were compared using their reported precursor-ion measurements,
177 chromatographic behavior, and available product-ion profiles. Similarity in precursor-ion
178 mass alone was not considered sufficient to establish molecular identity. Signals with
179 discrepant precursor-ion measurements or product-ion profiles were evaluated separately
180 unless their correspondence could be established from the available analytical records.
181 Although three biological replicates were prepared per isolate, the available summary
182 records did not establish the replicate-level occurrence of every selected molecular
183 feature. Accordingly, detection of a signal in an isolate was not interpreted as evidence
184 that it occurred consistently in all three biological replicates. No inferential statistical tests
185 or quantitative comparisons of molecular abundance were performed. The resulting
186 comparisons were used to describe the distribution of selected molecular features and
187 prioritize candidates for further characterization, rather than to establish definitive
188 molecular structures, biosynthetic pathways, or quantitative differences among isolates.

The complete set of supplementary chromatograms and mass spectra is provided in Online Resource 1 (Figs. S1–S59).

Results

Comparative molecular-feature profiling reveals distinct molecular patterns among Antarctic bacterial isolates

LC–MS analysis revealed distinct molecular-feature profiles among the five Antarctic bacterial isolates: *Arthrobacter cryoconiti* LAP 167 (A1), *Pseudomonas* sp. AT LP67 (B1), *Microbacterium* sp. LEMMJ01 (C7), and the two *Arthrobacter agilis* isolates F1 and G1 (Fig. 1). Detected signals were concentrated predominantly within the *m/z* 500–580 range, alongside additional features near *m/z* 628, 685, 699, 713, and 741 (Fig. 2). The profiles differed in the occurrence of individual features and, for selected signals, in chromatographic retention and MS/MS fragmentation patterns. To characterize these differences, selected features were compared using four complementary descriptors: precursor-ion mass, retention time, product-ion patterns, and occurrence across isolates. This integrated comparison enabled the identification of recurrent and isolate-restricted features and provided a basis for distinguishing signals with similar precursor-ion masses but different chromatographic or fragmentation characteristics. The corresponding chromatograms and mass spectra for the individual isolates are provided in Online Resource 1 (Figs. S1–S59).

Fig. 1 Chromatographic profiles of extracts from the five bacterial strains analyzed. Chromatograms obtained for strains A1 (*Arthrobacter cryoconiti* LAP 167), B1 (*Pseudomonas* sp. AT LP67), C7 (*Microbacterium* sp. LEMMJ01), F1 (*Arthrobacter agilis*), and G1 (*Arthrobacter agilis*) following liquid chromatographic separation. The profiles illustrate differences in the chromatographic signals detected among the strains

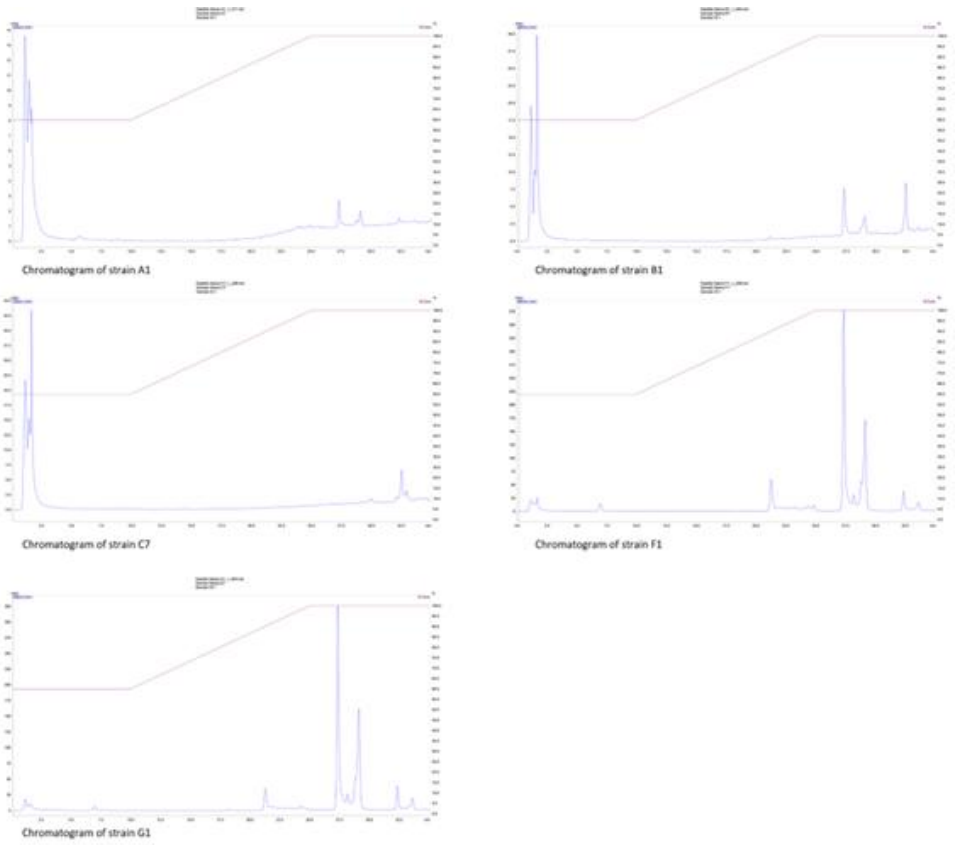
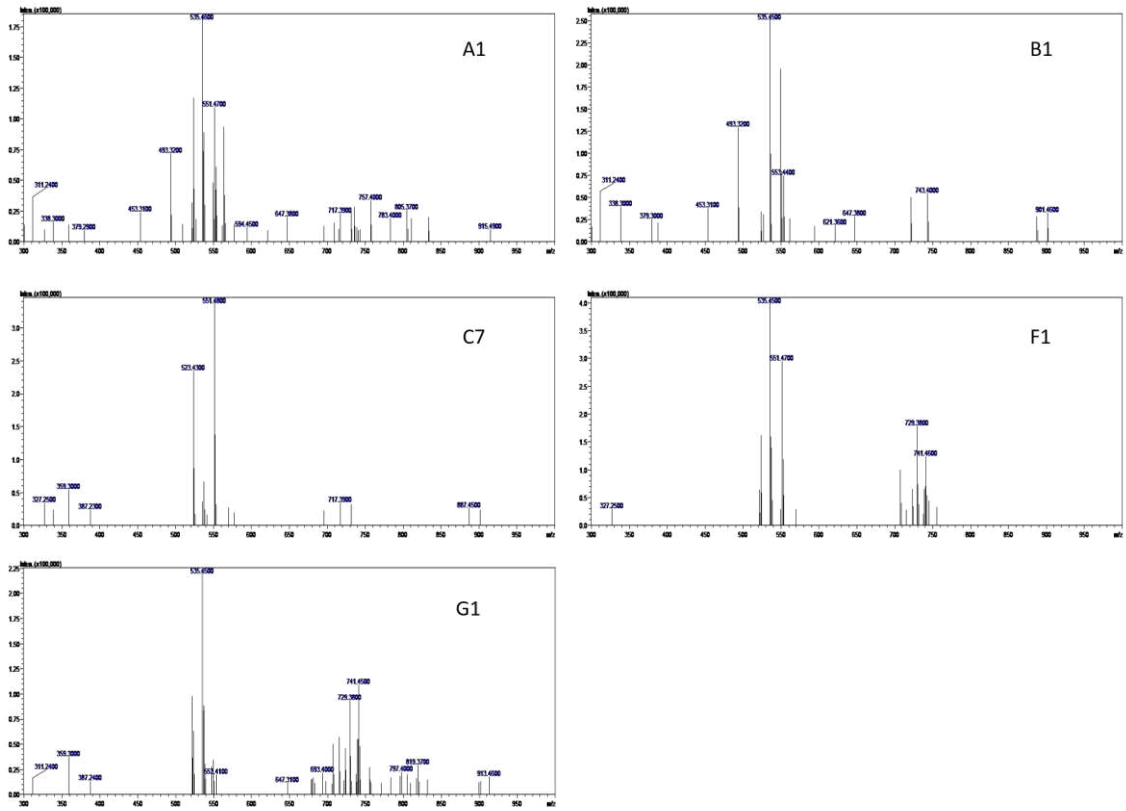


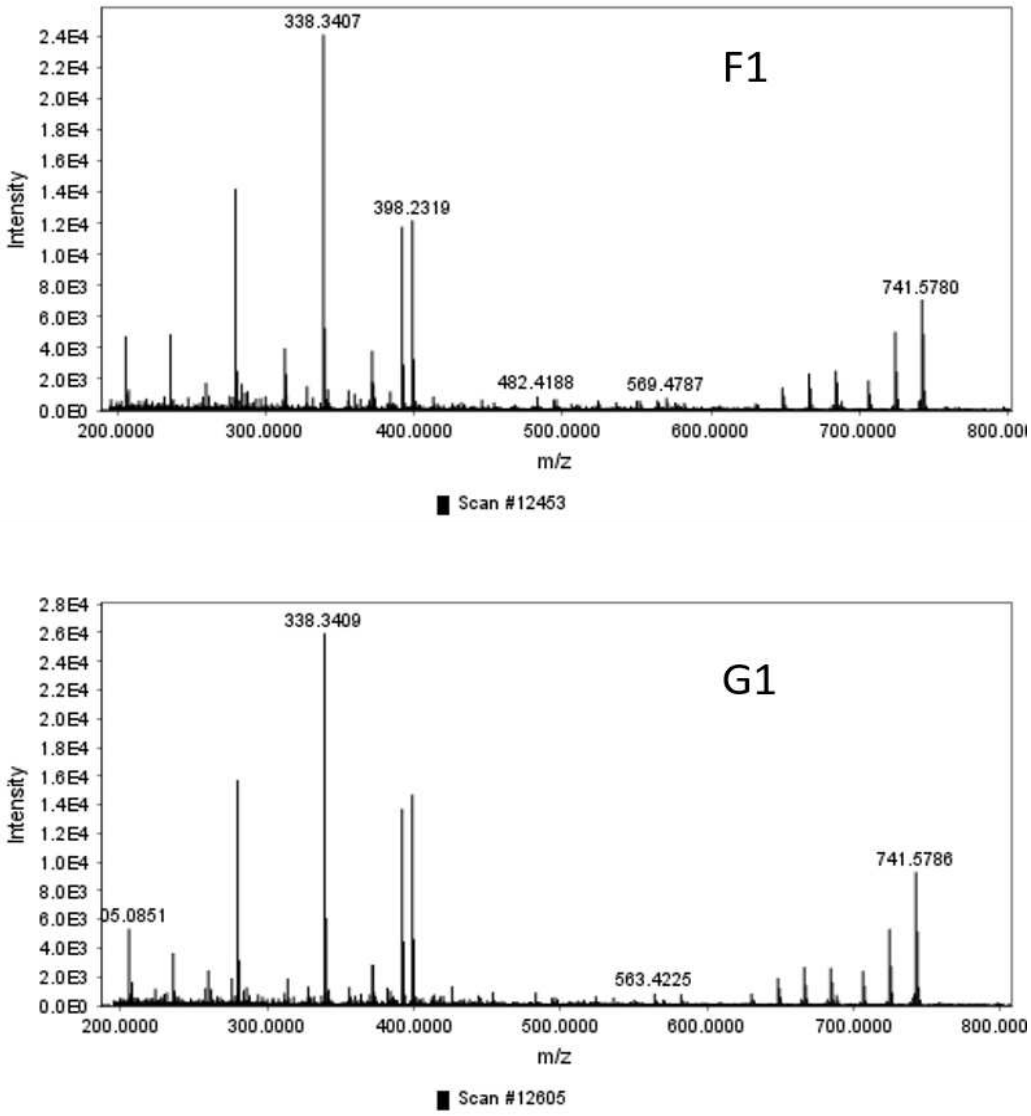
Fig. 2 Low-resolution mass spectrometric profiles of the bacterial extracts. Mass spectra obtained from the five bacterial strains, showing the distribution and relative intensities of the detected *m/z* signals. The spectra provide a comparative overview of the molecular features present in the extracts but do not independently establish compound identities



A shared molecular feature near m/z 741.578 in two *Arthrobacter agilis* isolates

A molecular feature near *m/z* 741.578 was detected in both *Arthrobacter agilis* isolates, F1 and G1. The reported precursor-ion masses were *m/z* 741.5780 for F1 and *m/z* 741.5786 for G1, differing by 0.0006 Da. Their MS/MS spectra contained closely matching product ions at *m/z* 338.3407 and 338.3409, respectively (Fig. 3). The spectrum for G1 is additionally provided in Supplementary Fig. S12. These observations support a close analytical correspondence between the two signals. However, the available evidence does not establish that they represent a specific molecular structure. The pink pigmentation of both isolates provides a biological context for investigating a possible association with carotenoid-related chemistry, consistent with reports of bacterioruberin in pink-pigmented *Arthrobacter* species (Flegler and Lipski 2022). Nevertheless, pigmentation and similarity in precursor-ion mass and product-ion signals are insufficient to identify the detected feature as bacterioruberin or another specific carotenoid. The signal is therefore described as an unresolved molecular feature with a possible carotenoid-related association. Further structural characterization is required to establish its chemical identity.

Fig. 3 Comparative MS/MS spectra of the unresolved molecular feature near *m/z* 741.578 detected in isolates F1 and G1. The spectra show precursor-ion signals at *m/z* 741.5780 (F1) and 741.5786 (G1), with closely matching reported product ions at *m/z* 338.3407 and 338.3409, respectively. These observations support analytical similarity between the two signals but do not establish their identity as bacterioruberin or another specific carotenoid

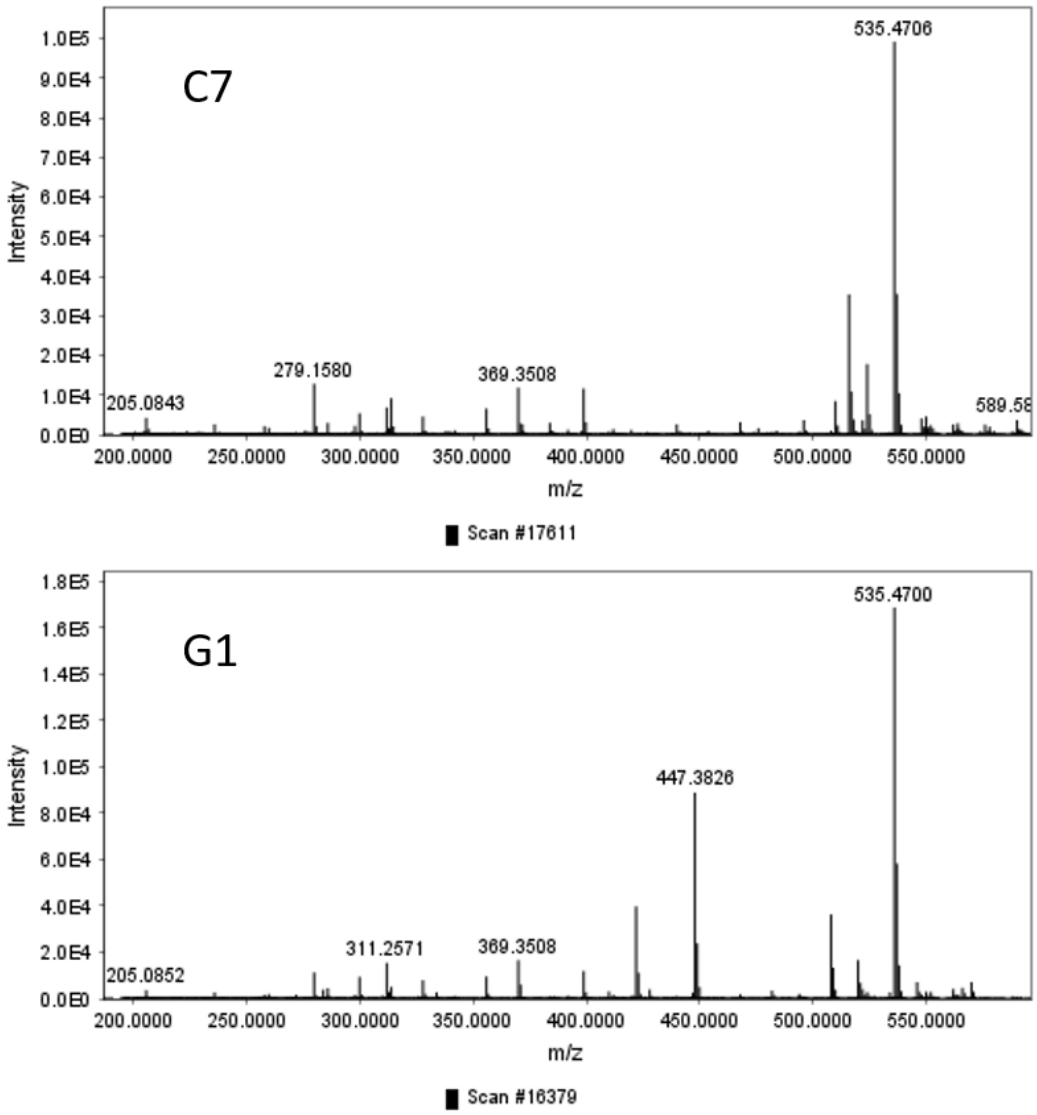


Differentiation of molecular features near m/z 535.470

Molecular features with closely similar precursor-ion *m/z* values were reported in *Microbacterium* sp. LEMMJ01 (C7) and the two *Arthrobacter agilis* isolates, G1 and F1. The reported precursor-ion values and retention times were *m/z* 535.4706 at 22.06 min for C7, *m/z* 535.4700 at 19.12 min for G1, and *m/z* 535.4704 at 19.30 min for F1. The corresponding MS/MS spectra are presented separately in Supplementary Fig. S33 (C7), Fig. S9 (G1), and Fig. S44 (F1). The C7 spectrum showed product ions at *m/z* 369.3508

and 279.1580, whereas the G1 spectrum showed product ions at *m/z* 447.3826, 369.3508, and 311.2571. The F1 spectrum in Supplementary Fig. S44 showed product ions at *m/z* 403.3566 and 299.2572. A second F1 record, Supplementary Fig. S46, reports a precursor ion at *m/z* 535.4697 and product ions at *m/z* 419.3506 and 279.1579; a retention time for this record is not established in the available summary. The two F1 records are therefore retained separately, and their product-ion lists are not combined. The MS/MS spectra of the C7 and G1 features are compared in Fig. 4. The available information does not establish whether they represent separate acquisitions of the same chromatographic feature or distinct features. Although the reported precursor-ion masses are closely similar, the retention times and product-ion profiles do not establish that the signals represent the same molecular structure. The previously considered molecular formula $C_{40}H_{54}$ is not compatible with these measurements under the proposed $[M+H]^+$ assignment: the theoretical *m/z* is approximately 535.4298, corresponding to a mass error of approximately 75 ppm relative to the reported precursor-ion signals. Accordingly, $C_{40}H_{54}$ was not retained as a valid molecular-formula assignment, and the signals cannot be classified as C_{40} carotenoids on this basis. Their molecular identities remain unresolved. Further structural assignment requires verification of the original precursor-ion measurements, ion and adduct assignments, and mass accuracy, followed by evaluation of candidate molecular formulas against diagnostic MS/MS evidence. No definitive carotenoid or diacylglycerol assignment is made for these features.

Fig. 4 Comparative MS/MS spectra of molecular features near *m/z* 535.470 detected in isolates C7 and G1. The C7 spectrum shows reported product ions at *m/z* 369.3508 and 279.1580, whereas the G1 spectrum shows product ions at *m/z* 447.3826, 369.3508, and 311.2571. Despite the similar precursor-ion masses and one shared reported product ion, the differences in fragmentation profiles do not establish that the two signals correspond to the same molecular structure

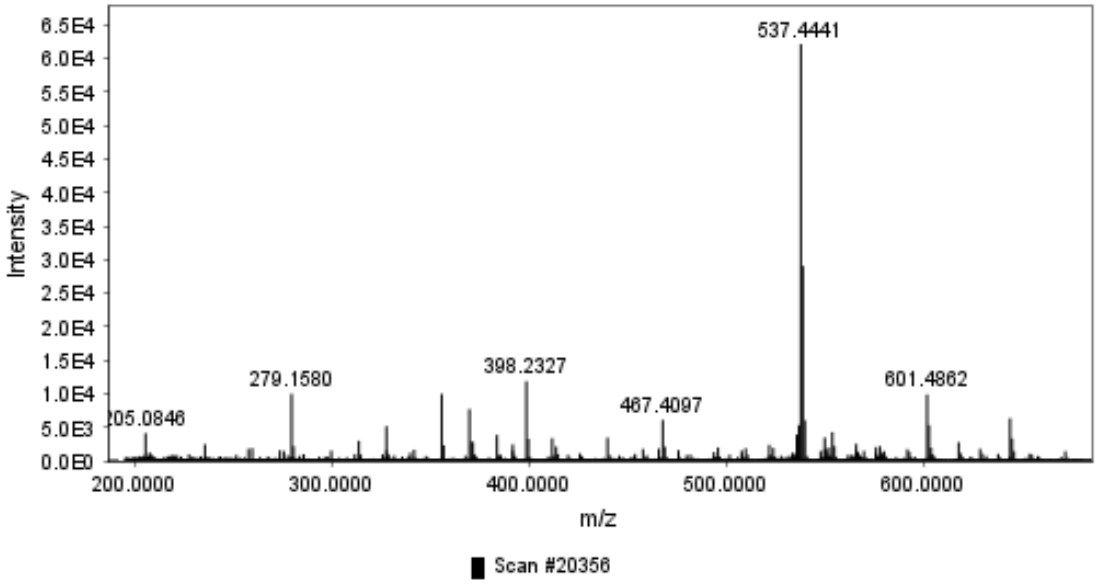


Comparison of bacterial molecular features with the β-carotene reference

The β-carotene reference exhibited a reported precursor ion at *m/z* 537.4441 under the analytical conditions employed (Fig. 5). A separate bacterial molecular feature near *m/z* 537.486 was reported in isolates A1, B1, C7, and F1. The reported precursor-ion value differed from that of the reference by approximately 0.0419 Da, corresponding to a mass difference of about 78 ppm relative to the reference value. This discrepancy does not support assigning the bacterial feature as β-carotene. The comparison therefore distinguishes the bacterial signal from the reference under the conditions employed but does not establish the identity of the bacterial feature. Its chemical structure remains unresolved and requires further investigation.

Fig. 5 High-resolution MS/MS spectrum of the β-carotene standard. The spectrum shows the reported precursor ion at *m/z* 537.4441 under the analytical conditions employed. The

standard provides an analytical reference for comparison with bacterial molecular features but does not independently establish their identities

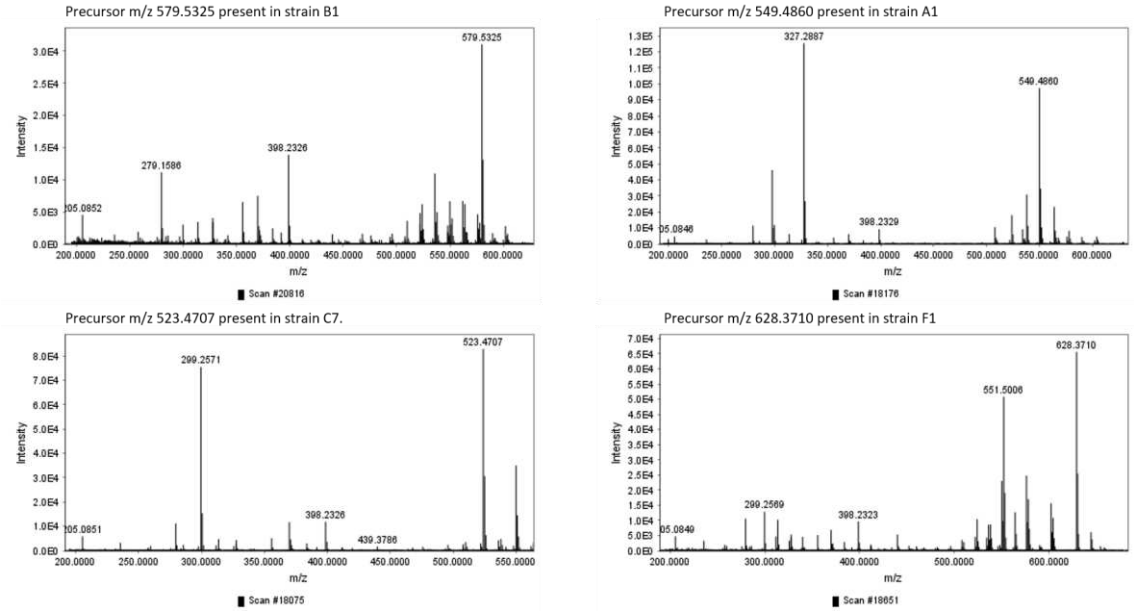


Integrated comparison of selected molecular features

The signals reported near *m/z* 509 and 521 were evaluated individually using their precursor-ion measurements and the corresponding supplementary MS/MS records. For the signals near *m/z* 509, Supplementary Fig. S22 reported a precursor ion at *m/z* 509.4549 in B1, whereas Supplementary Fig. S34 reported a precursor ion at *m/z* 509.4651 in C7. The difference of approximately 0.0102 Da does not support treating these measurements as a confirmed match. The two signals were therefore retained as separate analytical features. For comparison of additional selected molecular features, Fig. 6 presents the MS/MS spectra associated with precursor ions at *m/z* 579.5325 in B1, 549.4860 in A1, 523.4707 in C7, and 628.3710 in F1. The distribution and comparative analytical characteristics of these and other selected features across the five isolates are summarized in Table 1.

Fig. 6 High-resolution MS/MS spectra of four selected unresolved molecular features detected in Antarctic bacterial extracts. (A) B1, precursor ion at *m/z* 579.5325, with reported product ions at *m/z* 398.2326 and 279.1586 (Supplementary Fig. S17); (B) A1, precursor ion at *m/z* 549.4860, with reported product ions at *m/z* 327.2887 and 398.2329 (Supplementary Fig. S53); (C) C7, precursor ion at *m/z* 523.4707, with reported product ions at *m/z* 439.3786, 398.2326, and 299.2571 (Supplementary Fig. S32); and (D) F1,

precursor ion at *m/z* 628.3710, with reported product ions at *m/z* 551.5006, 398.2323, and 299.2569 (Supplementary Fig. S42). A separate feature detected in A1 at *m/z* 579.5324, with a different reported product-ion profile, is shown in Supplementary Fig. S52 and should not be conflated with panel A. These spectra support comparative analysis of fragmentation profiles but do not establish definitive molecular structures



Discussion

Comparative molecular profiles and biotechnological relevance

The LC–MS/MS comparison revealed overlapping but differentiated distributions of selected molecular features across the five Antarctic bacterial isolates. A signal near m/z 537.486 was reported in A1, B1, C7, and F1, a feature near m/z 523.470 in B1, C7, and G1, and closely matching precursor-ion features near m/z 741.578 in F1 and G1. Together, these patterns highlight both shared and isolate-associated features, providing a comparative basis for investigating molecular diversity among Antarctic bacteria. Although the present data do not establish quantitative differences in abundance or confirm that signals with similar precursor-ion values represent the same compound, their distribution provides a practical starting point for prioritizing candidates for further characterization. Previous studies have documented diverse pigment profiles and biological activities in Antarctic bacteria. Pradel et al. (2021) characterized a carotenoid mixture from the Antarctic isolate CN7, assigned to the genus *Flavobacterium* based on 16S rRNA gene sequence analysis. The sequence showed 99.3% identity to

Flavobacterium segetis AT1048, although the authors noted that additional genomic comparison was needed to confirm the species-level assignment. Their analysis detected multiple peaks in the carotenoid-absorption range, including a major signal consistent with lutein or zeaxanthin. Reis-Mansur et al. (2019) investigated pigments from Antarctic *Microbacterium* sp. LEMMJ01 and reported evidence that the pigment extract contributed to UV-B photoprotection, with mass-spectrometric signals consistent with neurosporene. These studies illustrate how the characterization of Antarctic bacterial pigments can reveal chemical diversity and potential biological relevance. In this context, the present study contributes a comparative overview of selected molecular features and identifies candidates that could be prioritized for structural characterization and subsequent evaluation of pigment yield, stability, and biological properties. Such applications remain prospective, as the present work did not quantify individual pigment yields, test purified compounds, or assess production scalability.

Closely matching precursor-ion features in the two *A. agilis* isolates

The F1 and G1 isolates exhibited precursor-ion signals at m/z 741.5780 and 741.5786, respectively, differing by 0.81 ppm relative to their mean. Assuming that both signals correspond to singly charged protonated molecules ($[M+H]^+$), the candidate formula $C_{50}H_{76}O_4$ has a calculated m/z of approximately 741.5816. The corresponding mass errors are −4.90 ppm for F1 and −4.10 ppm for G1. Both values fall within the ±5 ppm screening criterion described in the Methods, although the F1 value is close to the acceptance limit. This agreement supports $C_{50}H_{76}O_4$ as a candidate formula under the proposed ion assignment, but does not establish the molecular formula or structure of the detected compound. Bacterioruberin has the molecular formula $C_{50}H_{76}O_4$ and has been reported in pink-pigmented *Arthrobacter* species, including *A. agilis* (Flegler and Lipski 2022a, 2022b; Noby et al. 2023). In a gene-silencing study, suppression of bacterioruberin biosynthesis in *Arthrobacter agilis* and *Arthrobacter bussei* was associated with reduced biomass production and growth rates at low temperatures (Flegler and Lipski 2022a). A separate study associated increased bacterioruberin content with altered membrane fluidity and greater resistance to freeze–thaw stress (Flegler and Lipski 2022b). These findings provide a biological rationale for investigating bacterioruberin in the Antarctic isolates. The close correspondence between the F1 and G1 precursor-ion signals, together with the established occurrence of bacterioruberin in *Arthrobacter*, identifies this feature as a relevant target for further investigation. The reported product ion at m/z 338.34

requires additional verification before it can contribute to structural interpretation. Examination of the original MS/MS data and precursor-isolation records will help clarify its relationship to the precursor and guide subsequent formula evaluation. Accordingly, the F1 and G1 signals provide a promising starting point for targeted characterization, with $C_{50}H_{76}O_4$ retained as a candidate formula and bacterioruberin as a biologically motivated hypothesis.

Interpretation of features near m/z 535.470 and 537.486

The signals reported near m/z 535.470 in C7, G1, and F1 do not support the candidate formula $C_{40}H_{54}$ under the proposed $[M+H]^+$ assignment. The calculated protonated-ion value for $C_{40}H_{54}$ is approximately m/z 535.4298, whereas the observed values were m/z 535.4706 for C7, 535.4700 for G1, and 535.4704 for F1. These measurements correspond to mass errors of approximately +76.15, +75.03, and +75.77 ppm, respectively, substantially exceeding the ±5 ppm screening criterion. The $C_{40}H_{54}$ annotation should therefore be withdrawn, and no alternative formula or specific compound should be assigned without reassessing the original precursor-ion records. The similar precursor-ion values do not independently establish a shared molecular identity. The reported retention times differed among C7 (22.06 min), G1 (19.12 min), and F1 (19.30 min), and the available product-ion profiles did not establish a common fragmentation pattern. A second F1 record also showed a different product-ion profile. The records should therefore remain separate unresolved features until their relationship can be evaluated from the original chromatographic and tandem mass-spectrometry data. The bacterial feature reported near m/z 537.486 in A1, B1, C7, and F1 is also inconsistent with β-carotene under the proposed $[M+H]^+$ assignment. The calculated protonated-ion value for β-carotene ($C_{40}H_{56}$) is approximately m/z 537.4455, and the reference standard was measured at m/z 537.4441, corresponding to a mass error of approximately −2.56 ppm. In contrast, the bacterial feature differs from the theoretical value by approximately +75.40 ppm and from the measured standard by approximately 78.0 ppm. These discrepancies do not support assigning the bacterial feature as β-carotene, but neither identify an alternative compound nor explain the cause of the difference. The original bacterial spectra, extracted-ion assignments, calibration records, and precursor-ion/adduct assignments must be checked before assigning a molecular identity. The differing MS/MS records for A1 and B1 also do not establish that these signals represent the same molecule. Together, these comparisons demonstrate the value of integrating

accurate mass, retention time, fragmentation patterns, and reference-standard measurements to distinguish molecular features across isolates. Although the identities of the signals near m/z 535.470 and 537.486 remain to be established, their analytical differences help define priorities for data verification and targeted structural characterization.

Distribution of other unresolved molecular features across the isolates

Other selected signals further illustrate the molecular diversity captured by the comparative analysis. Signals near m/z 509.455 in B1 and 509.465 in C7 were retained separately because their precursor-ion values differed. Signals near m/z 521.455 in B1, G1, and A1 were provisionally grouped by precursor-ion mass, whereas the F1 signal at m/z 521.4646 was treated separately. A feature near m/z 523.470 was reported in B1, C7, and G1, and additional signals near m/z 549.486, 579.533, and 628.371 were observed. The distributions of these features reveal both overlapping and isolate-associated patterns that can guide selection of targets for subsequent characterization. The chemical identities of these additional signals remain unresolved, and the available evidence does not establish specific diacylglycerol species, fatty-acyl compositions, or other defined lipid structures. Nevertheless, organizing the features according to their precursor-ion measurements, chromatographic behavior, and available product-ion profiles provides a useful framework for comparing the isolates and distinguishing provisional analytical groupings from stronger evidence of structural correspondence. Follow-up analysis should prioritize features for which additional spectral evidence or suitable reference compounds could most effectively resolve the remaining uncertainty.

Study limitations and future directions

This study was exploratory and focused on selected features with available analytical records rather than comprehensive untargeted metabolomics. Although three biological replicates were prepared per isolate, replicate-level detection was not established for every feature, and no inferential tests or quantitative abundance comparisons were performed. The reported distributions therefore describe the selected analytical observations rather than demonstrating consistent detection across replicates or quantitative differences among isolates. β-Carotene was the only direct reference standard described, and most features were not structurally identified. These limitations define the

scope of the conclusions while leaving a clear basis for targeted follow-up. The next stage should begin with an audit of the original acquisition files and calibration records for the features near m/z 741.578, 535.470, and 537.486, including precursor-ion values, charge states, extracted-ion assignments, and possible adducts. The precursor-isolation and product-ion records associated with m/z 338.34 require particular attention because their verification will determine how the F1 and G1 signals can be interpreted. Following this audit, documented feature detection, chromatographic alignment, quality-control procedures, and replicate-level comparisons could help establish the reproducibility of the observed distributions. Targeted MS/MS at multiple collision energies, curated spectral-library comparisons, and appropriate authentic standards could strengthen structural assignments. UV–visible or diode-array spectra could provide complementary evidence for pigment candidates, while isolation followed by NMR could be considered if sufficient material were available. Reliable annotation requires integrating accurate precursor mass with consistent ion/adduct assignments, chromatographic behavior, interpretable product-ion spectra, and comparison with reference data or authentic standards (Azevedo-Meleiro and Rodriguez-Amaya 2004; Rivera et al. 2014; Sandmann 2022; López et al. 2023). Metz et al. (2025) further discuss identification probability as a way to express ambiguity in metabolite annotation. Overall, this study establishes a comparative framework for investigating selected molecular features across five Antarctic bacterial isolates. By describing shared and isolate-associated patterns and identifying priorities for structural follow-up, the findings provide a foundation for further investigation of bacterial pigment diversity and its potential biotechnological relevance. Subsequent confirmation of molecular identities and evaluation of biological properties will determine which candidates warrant more detailed functional and application-oriented studies.

Conclusion and Future Perspectives

Comparative LC-MS and LC-HR-Q-TOF-MS/MS profiling of five Antarctic bacterial isolates revealed overlapping but differentiated distributions of selected molecular features. The feature near *m/z* 537.486 showed the broadest reported distribution, occurring in four isolates, whereas the feature near *m/z* 741.578 was detected in both *Arthrobacter agilis* isolates. Signals near *m/z* 535.470 exhibited similar precursor-ion masses but different reported chromatographic and MS/MS characteristics,

highlighting the importance of evaluating multiple analytical descriptors when comparing molecular features.

The comparison with an experimental β-carotene reference distinguished the bacterial signal near *m/z* 537.486 from the standard under the conditions employed. However, the available evidence did not establish specific carotenoid structures, C40 or C50 classifications, or individual diacylglycerol species. In addition, discrepancies among selected precursor-ion records require reconciliation before the corresponding features can be considered analytically consistent across isolates. The principal contribution of this study is therefore a comparative characterization of selected molecular features and their distribution across the isolate collection, rather than definitive molecular identification. Further work should prioritize verification of precursor-ion and adduct assignments, consistent interpretation of individual MS/MS spectra, and structural confirmation using diagnostic fragmentation, appropriate reference data, and authentic standards where available. Quantitative or functional conclusions will require dedicated analyses beyond the descriptive comparisons presented here.

Declarations

Ethical Approval

Not applicable.

Funding

This work was supported by the São Paulo Research Foundation (FAPESP, Brazil; grant numbers 2023/18416-0, 2025/18237-4, and 2023/13870-5), the National Council for Scientific and Technological Development (CNPq, Brazil; grant numbers 303952/2024-5, 407743/2024-3, and 305353/2023-3), and the Coordination for the Improvement of Higher Education Personnel (CAPES, Brazil).

Competing Interests

The authors declare that they have no competing interests.

Availability of Data and Materials

The data supporting the findings of this study, including chromatographic and mass spectrometric data, selected MS/MS spectra, and the mapping of reported molecular features to the corresponding isolates and supplementary figures, are available from the corresponding author upon reasonable request.

References

Akulava V, Byrtusova D, Zimmermann B, Smirnova M, Kohler A, Miamin U, Valentovich L, Shapaval V (2024) Screening for pigment production and characterization of pigment profile and photostability in cold-adapted Antarctic bacteria using FT-Raman spectroscopy. J Photochem Photobiol A Chem 450:115461. https://doi.org/10.1016/j.jphotochem.2024.115461

Al-Monofy KB, Farghali MH, Al-Madboly LA, Abo Kamer AM, Abdelaziz AA (2025) Advances in biomanufacturing and recent biological applications of the fundamental bacterial carotenoids: a comprehensive review. Microb Cell Fact 24:225. https://doi.org/10.1186/s12934-025-02847-1

Ashokkumar V, Flora G, Sevanan M, Sripriya R, Chen WH, Park J-H, Banu JR, Kumar G (2023) Technological advances in the production of carotenoids and their applications—a critical review. Bioresour Technol 367:128215. https://doi.org/10.1016/j.biortech.2022.128215

Azevedo-Meleiro CH, Rodriguez-Amaya DB (2004) Confirmation of the identity of the carotenoids of tropical fruits by HPLC-DAD and HPLC-MS. J Food Compos Anal 17:385–396. https://doi.org/10.1016/j.jfca.2004.02.004

Ben Hamad Bouhamed S, Chaari M, Baati H, Zouari S, Ammar E (2024) Extreme halophilic *Archaea*: *Halobacterium salinarum* carotenoids characterization and antioxidant properties. Heliyon 10:e36832. https://doi.org/10.1016/j.heliyon.2024.e36832

Bertani G (1951) Studies on lysogenesis. I. The mode of phage liberation by lysogenic *Escherichia coli*. J Bacteriol 62:293–300. https://doi.org/10.1128/jb.62.3.293-300.1951

Flegler A, Lipski A (2022a) The C50 carotenoid bacterioruberin regulates membrane fluidity in pink-pigmented *Arthrobacter* species. Arch Microbiol 204:70. https://doi.org/10.1007/s00203-021-02719-3

Flegler, A., & Lipski, A. (2022b). Engineered CRISPR/Cas9 system for transcriptional gene silencing in *Arthrobacter* species indicates bacterioruberin is indispensable for

growth at low temperatures. Current Microbiology, 79(7), Article 199. https://doi.org/10.1007/s00284-022-02887-5

Korkerd S, Vatanyoopaisarn S, Visessanguan W, Thumthanarak B, Uttapap D, Mussatto SI, Rungsardthong V (2024) Screening, identification, and characterization of high potential bacteria for β-cryptoxanthin production from natural sources. Biocatal Agric Biotechnol 57:103089. https://doi.org/10.1016/j.bcab.2024.103089

Krakko D, Tautenhahn R, Stutts WL (2026) Implementing annotation confidence scoring in untargeted mass spectrometry workflows for small molecule analysis. Anal Chem 98:10352–10359. https://doi.org/10.1021/acs.analchem.5c03229

Li S, Tang X, Lu Y, Xu J, Chen J, Chen H (2021) An improved method for the separation of carotenoids and carotenoid isomers by liquid chromatography–mass spectrometry. J Sep Sci 44:539–548. https://doi.org/10.1002/jssc.202000902

López GD, Álvarez-Rivera G, Carazzone C, Ibáñez E, Leidy C, Cifuentes A (2023) Bacterial carotenoids: extraction, characterization, and applications. Crit Rev Anal Chem 53:1239–1262. https://doi.org/10.1080/10408347.2021.2016366

Maoka T (2023) Carotenoids: distribution, function in nature, and analysis using LC-photodiode array detector (DAD)-MS and MS/MS system. Mass Spectrom 12:A0133. https://doi.org/10.5702/massspectrometry.A0133

Medeiros W, Kralova S, Oliveira V, Ziemert N, Sehnal L (2025) Antarctic bacterial natural products: from genomic insights to drug discovery. Nat Prod Rep 42:774–787. https://doi.org/10.1039/d4np00045e

Metz TO, Chang CH, Gautam V, Anjum A, Tian S, Wang F, Colby SM, Nunez JR, Blumer MR, Edison AS, Fiehn O, Jones DP, Li S, Morgan ET, Patti GJ, Ross DH, Shapiro MR, Williams AJ, Wishart DS (2025) Introducing "identification probability" for automated and transferable assessment of metabolite identification confidence in metabolomics and related studies. Anal Chem 97:1–11. https://doi.org/10.1021/acs.analchem.4c04060

Naik R, Gupte S (2024) Characterization of pigment produced by high carotenoid yielding bacteria *Paracoccus marcusii* RSPO1 and evaluation of its anti-diabetic, anti-

microbial and antioxidant properties. Nat Prod Res 38:968–977. https://doi.org/10.1080/14786419.2023.2208358

Noby N, Khattab SN, Soliman NA (2023) Sustainable production of bacterioruberin carotenoid and its derivatives from *Arthrobacter agilis* NP20 on whey-based medium: optimization and product characterization. Bioresour Bioprocess 10:46. https://doi.org/10.1186/s40643-023-00662-3

Palanisamy M, Ramalingam S (2024) Microbial bacterioruberin: a comprehensive review. Indian J Microbiol 64:1477–1501. https://doi.org/10.1007/s12088-024-01312-8

Paredes Contreras BV, Vermelho AB, Casanova L, Lage CAS, Vilela CLS, Cardoso VS, Arge LWP, Cardoso-Rurr JS, Correa SS, De Mansoldo FRP, Reis-Mansur MCPP, da Silva EA, Schultz J, Rosado AS (2025) Enhanced UV-B photoprotection activity of carotenoids from the novel *Arthrobacter* sp. strain LAPM80 isolated from King George Island, Antarctica. Heliyon 11:e41400. https://doi.org/10.1016/j.heliyon.2024.e41400

Polyakov NE, Focsan AL, Gao Y, Kispert LD (2023) The endless world of carotenoids—structural, chemical and biological aspects of some rare carotenoids. Int J Mol Sci 24:9885. https://doi.org/10.3390/ijms24129885

Pradel P, Calisto N, Navarro L, Barriga A, Vera N, Aranda C, Simpfendorfer R, Valdés N, Corsini G, Tello M, González AR (2021) Carotenoid cocktail produced by an Antarctic soil *Flavobacterium* with biotechnological potential. Microorganisms 9:2419. https://doi.org/10.3390/microorganisms9122419

Reis-Mansur MCPP, Cardoso-Rurr JS, Silva JVMA, Rodrigues de Souza G, Cardoso VS, Passos Mansoldo FR, Pinheiro Y, Schultz J, Lopez Balottin LB, Ribeiro da Silva AJ, Lage C, Pereira dos Santos E, Soares Rosado A, Vermelho AB (2019) Carotenoids from UV-resistant Antarctic *Microbacterium* sp. LEMMJ01. Sci Rep 9:9554. https://doi.org/10.1038/s41598-019-45840-6

Rivera SM, Christou P, Canela-Garayoa R (2014) Identification of carotenoids using mass spectrometry. Mass Spectrom Rev 33:353–372. https://doi.org/10.1002/mas.21390

Sandmann G (2022) HPLC analysis of carotenoids from bacteria. In: Wurtzel ET (ed) Carotenoids: carotenoid and apocarotenoid analysis. Methods in Enzymology, vol 670. Academic Press, pp 139–153. https://doi.org/10.1016/bs.mie.2021.10.006

Scales BS, Hassenrück C, Moldaenke L, Hassa J, Rückert-Reed C, Rummel C, Völkner C, Rynek R, Busche T, Kalinowski J, Jahnke A, Schmitt-Jansen M, Wendt-Potthoff K, Oberbeckmann S (2024) Hunting for pigments in bacterial settlers of the Great Pacific Garbage Patch. Environ Microbiol 26:e16639. https://doi.org/10.1111/1462-2920.16639

Schmid R, Heuckeroth S, Korf A, Smirnov A, Myers O, Dyrlund TS, Bushuiev R, Murray KJ, Hoffmann N, Lu M, Sarvepalli A, Zhang Z, Fleischauer M, Dührkop K, Wesner M, Hoogstra SJ, Rudt E, Mokshyna O, Brungs C, Ponomarov K, Mutabdžija L, Damiani T, Pudney CJ, Earll M, Helmer PO, Fallon TR, Schulze T, Rivas-Ubach A, Bilbao A, Richter H, Nothias L-F, Wang M, Orešič M, Weng J-K, Böcker S, Jeibmann A, Hayen H, Karst U, Dorrestein PC, Petras D, Du X, Pluskal T (2023) Integrative analysis of multimodal mass spectrometry data in MZmine 3. Nat Biotechnol 41:447–449. https://doi.org/10.1038/s41587-023-01690-2

Schultz J, de Souza YAP, Mansur MCPPR, Vermelho AB, da Mota FF, Rosado AS (2017) Draft genome sequence of *Microbacterium* sp. strain LEMMJ01, isolated from Antarctic ornithogenic soil. Genome Announc 5:e00672-17. https://doi.org/10.1128/genomeA.00672-17

Silva AC da, Rachid CTCDC, de Jesus HE, Rosado AS, Peixoto RS (2017) Predicting the biotechnological potential of bacteria isolated from Antarctic soils, including the rhizosphere of vascular plants. Polar Biol 40:1393–1407. https://doi.org/10.1007/s00300-016-2065-0

Silva TR, Tavares RSN, Canela-Garayoa R, Eras J, Rodrigues MVN, Neri-Numa IA, Pastore GM, Rosa LH, Schultz JAA, Debonsi HM, Cordeiro LRG, Oliveira VM (2019) Chemical characterization and biotechnological applicability of pigments isolated from Antarctic bacteria. Mar Biotechnol 21:416–429. https://doi.org/10.1007/s10126-019-09892-z

Styczynski M, Rogowska A, Gieczewska K, Garstka M, Szakiel A, Dziewit L (2020) Genome-based insights into the production of carotenoids by Antarctic bacteria,

Planococcus sp. ANT_H30 and *Rhodococcus* sp. ANT_H53B. Molecules 25:4357. https://doi.org/10.3390/molecules25194357

Vila E, Hornero-Méndez D, Azziz G, Lareo C, Saravia V (2019) Carotenoids from heterotrophic bacteria isolated from Fildes Peninsula, King George Island, Antarctica. Biotechnol Rep 21:e00306. https://doi.org/10.1016/j.btre.2019.e00306

Tables

Table 1. Comparative distribution and analytical characterization of selected molecular features across five Antarctic bacterial isolates

Feature (*m/z*)	Isolate(s)	Comparative designation	Retention time (min)	Analytical interpretation
741.578	F1, G1	Recurring analytically similar feature	23.23–23.42	Reported in both *Arthrobacter agilis* isolates, with closely matching precursor-ion masses, retention times, and a product ion near *m/z* 338.3408. The recurrence supports further structural characterization. A carotenoid-related association remains hypothetical; neither a specific structure nor a C50 classification has been established.
537.486	A1, B1, C7, F1	Feature reported in four isolates	22.89; 23.10; 22.81; 22.63	Reported in four of the five isolates. Its precursor-ion mass and retention behavior differ from those of the β-carotene reference under the conditions employed. Its molecular identity remains unresolved.
535.470	F1	F1-associated analytical feature	19.30	Reported at 19.30 min. A second F1 MS/MS record reports a similar precursor-ion mass but a different product-ion profile. The relationship between the records remains unresolved; their product-ion lists are not combined.
535.470	C7, G1	Differentiated features with similar precursor-ion masses	22.06; 19.12	The C7 and G1 signals differ in retention time and reported product-ion profiles. The available evidence does not establish a common molecular identity or a definitive carotenoid or diacylglycerol assignment.
523.470	B1, C7, G1	Feature reported in three isolates	22.16; 22.31; 21.98	Reported in three isolates. This distribution supports comparative analysis, but the chemical identity and any specific lipid-class assignment remain unresolved.
521.455	B1, G1, A1	Provisional grouping by	21.57; 20,98; 21.19	The reported precursor-ion values are 521.4546 (B1), 521.4548 (G1), and 521.4553 (A1). Their mass

		precursor-ion mass		agreement supports a provisional analytical grouping but does not establish molecular identity. The retention time for B1 requires verification from the original chromatographic records.
521.465	F1	Separately reported feature	18.45	Supplementary Fig. S47 reports a precursor ion at *m/z* 521.4646. This signal is excluded from the provisional grouping near m/z 521.455 pending verification.
509.455	B1	B1-associated analytical feature	21.71	Supplementary Fig. S22 reports a precursor ion at *m/z* 509.4549. Its correspondence with the C7 signal has not been established.
509.465	C7	Separately reported feature	21.64	Supplementary Fig. S34 reports a precursor ion at *m/z* 509.4651. It is not treated as a confirmed match to the B1 feature.

Abbreviations: MS/MS, tandem mass spectrometry; *m/z*, mass-to-charge ratio.

Supplementary Files

This is a list of supplementary files associated with this preprint. Click to download.

- ESM1.pdf